

Large magnetoresistance of a dilute p -Si/SiGe/Si quantum well in a parallel magnetic field

I. L. Drichko,¹ I. Yu. Smirnov,^{1,*} A. V. Suslov,² O. A. Mironov,³ and D. R. Leadley⁴

¹*A. F. Ioffe Physico-Technical Institute, Russian Academy of Sciences, 194021 St. Petersburg, Russia*

²*National High Magnetic Field Laboratory, Tallahassee, Florida 32310, USA*

³*Warwick SEMINANO R&D Centre, University of Warwick Science Park, Coventry CV4 7EZ, United Kingdom*

⁴*Department of Physics, University of Warwick, Coventry CV4 7AL, United Kingdom*

(Received 10 December 2008; revised manuscript received 14 April 2009; published 11 May 2009)

We report the results of an experimental study of the magnetoresistance ρ_{xx} in two samples of p -Si/SiGe/Si with low carrier concentrations $p=8.2 \times 10^{10} \text{ cm}^{-2}$ and $p=2 \times 10^{11} \text{ cm}^{-2}$. The research was performed in the temperature range of 0.3–2 K in the magnetic fields of up to 18 T, parallel to the two-dimensional (2D) channel plane at two orientations of the in-plane magnetic field B_{\parallel} against the current I : $B_{\parallel} \perp I$ and $B_{\parallel} \parallel I$. In the sample with the lowest density in the magnetic field range of 0–7.2 T, the temperature dependence of ρ_{xx} demonstrates the metallic characteristics ($d\rho_{xx}/dT > 0$). However, at $B_{\parallel}=7.2$ T the derivative $d\rho_{xx}/dT$ reverses the sign. Moreover, the resistance depends on the current orientation with respect to the in-plane magnetic field. At $B_{\parallel} \cong 13$ T there is a transition from the dependence $\ln(\Delta\rho_{xx}/\rho_0) \propto B_{\parallel}^2$ to the dependence $\ln(\Delta\rho_{xx}/\rho_0) \propto B_{\parallel}$. The observed effects can be explained by the influence of the in-plane magnetic field on the orbital motion of the charge carriers in the quasi-2D system.

DOI: 10.1103/PhysRevB.79.205310

PACS number(s): 73.23.-b, 73.43.Qt

I. INTRODUCTION

Large positive magnetoresistance in two-dimensional systems in the in-plane magnetic field is typically explained by a modification in the spin system of the charge carriers. Studies of the in-plane field-induced magnetoresistance were conducted in numbers of low-density heterostructures n -Si silicon metal-oxide-semiconductor field-effect transistors (MOSFETs),¹ n -Si/SiGe,² n -GaAs/AlGaAs,³ p -GaAs/AlGaAs,^{3–5} and n -Al_{0.4}Ga_{0.6}As/AlAs/Al_{0.4}Ga_{0.6}As.³ Indeed, within the narrow quantum well approximation the orbital motion of the charge carriers is suppressed, but the Zeeman splitting $g^* \mu_B B$ lifts spin degeneracy, where g^* is the effective g factor, μ_B is the Bohr magneton, and B is the total magnetic field. Thus, when the magnetic field is rising the conduction band is being split into two subbands with the opposite spin directions and, finally, all spin-down electrons find themselves in the bottom subband under the Fermi level. Consequently, the electronic system becomes completely spin polarized. As a rule, in the magnetic fields exceeding a critical value corresponding to the field of full spin polarization, a saturation of resistance is observed.^{1–4} Several spin-effect-based theories were developed to interpret the nature of positive magnetoresistance.^{6–9}

However, in some studies on n - and p -GaAs/AlGaAs (Refs. 3 and 5) no saturation of the magnetoresistance was observed. Authors of the theory in Ref. 10 interpreted that experimental fact by coupling of the in-plane field to the carrier orbital motion due to the finite thickness of the two-dimensional (2D) layer. Validity of such a model proves to be true experimentally: unlike cases of Refs. 3 and 5 where the investigated samples p -GaAs/AlGaAs by all appearances had a *wide* quantum well, in p -GaAs/AlGaAs with the *narrow* quantum well a distinct saturation of positive magnetoresistance was observed.⁴

It is worth noting that positive magnetoresistance in parallel magnetic fields was observed in dilute carrier systems

only. In the system under study p -Si/Si_{1-x}Ge_x/Si a quantum well formed in the strained Si_{1-x}Ge_x is asymmetrical due to only one of the silicon barriers to be boron doped. The three-fold (not considering a spin) degenerated valence band of SiGe is split into three subbands due to a strong spin-orbit interaction and a strain.¹¹ The top subband occupied by heavy holes is formed by the states with quantum numbers $L=1$, $S=1/2$, and $J=3/2$. As a result, there is a strong anisotropy of the g factor with respect to the magnetic field orientation: $g_{\perp}^* \cong 4.5$ when a magnetic field is applied perpendicular to the quantum well plane, and $g_{\parallel}^* \cong 0$ when the field is oriented in the plane of the 2D channel.¹² Thus, the Zeeman spin splitting in a parallel field is small. Considering this fact several authors, for example,^{13,14} stated that effect of an in-plane magnetic field on the resistance in this material has to be very weak. That opinion was based also on a few experiments¹⁴ carried out on the p -Si/SiGe systems with $p=2.5 \times 10^{11} \text{ cm}^{-2}$. The experimental results presented below show that a parallel magnetic field still greatly affects the resistance in the low-density p -Si/SiGe/Si quantum well despite the lack of the spin effect.

II. EXPERIMENT AND DISCUSSION

The dc magnetoresistance ρ_{xx} was measured in the in-plane magnetic field on two p -Si/SiGe/Si quantum wells, with the carrier densities $p=8.2 \times 10^{10} \text{ cm}^{-2}$ and $p=2 \times 10^{11} \text{ cm}^{-2}$, respectively, and a hole mobility of $\mu=1 \times 10^4 \text{ cm}^2/\text{V}\cdot\text{s}$ at liquid-helium temperatures. The studies were performed in the fields of up to 18 T and in the temperature range of 0.3–2 K at two orientations of the in-plane magnetic field B_{\parallel} with respect to the current I : $B_{\parallel} \perp I$ and $B_{\parallel} \parallel I$.

The 2D-system Si(B)/Si/SiGe/Si/(001)Si was grown in Warwick on a Si (001) substrate by the solid source molecular-beam epitaxy. It consisted of the 300 nm Si buffer layer followed by 30 nm Si_{0.92}Ge_{0.08} layer (sample with

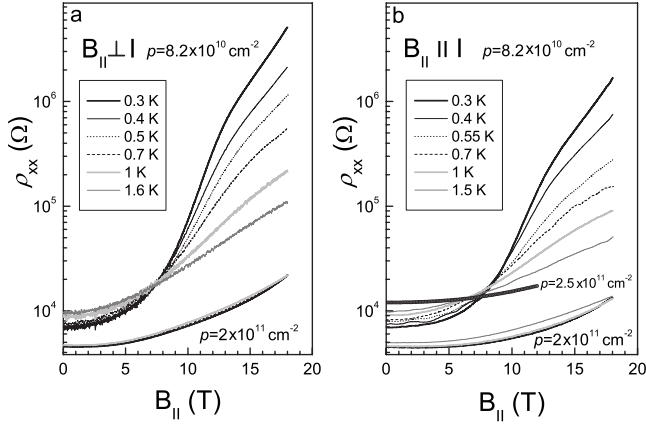


FIG. 1. Magnetoresistance ρ_{xx} versus $B_{||}$ parallel to the two-dimensional system for the samples with $p=8.2 \times 10^{10} \text{ cm}^{-2}$ and $p=2 \times 10^{11} \text{ cm}^{-2}$ with two B -to- I orientations: (a) $B_{||} \perp I$ and (b) $B_{||} || I$; the curve for $p=2.5 \times 10^{11} \text{ cm}^{-2}$ at $T=0.5 \text{ K}$ is the result of Ref. 14.

$p=8.2 \times 10^{10} \text{ cm}^{-2}$) or $\text{Si}_{0.87}\text{Ge}_{0.13}$ layer (sample with $p=2 \times 10^{11} \text{ cm}^{-2}$), and 20 nm undoped spacer and 50 nm layer of B-doped Si with doping concentration $2.5 \times 10^{18} \text{ cm}^{-3}$. Magnetoresistance of the sample with $p=8.2 \times 10^{10} \text{ cm}^{-2}$ was studied in detail earlier in wide range of transverse magnetic fields and temperatures.¹⁵ At the field $B=0 \text{ T}$ the resistance in both samples demonstrated a metallic behavior.

Figure 1 illustrates dependences of the resistance ρ_{xx} on the in-plane magnetic field $B_{||}$ at various temperatures. It is evident that $\rho_{xx}(B_{||})$ curves related to the sample with $p=8.2 \times 10^{10} \text{ cm}^{-2}$, while been measured at different temperatures, cross at a single point corresponding to $B_{||} \approx 7.2 \text{ T}$ and $\rho_{xx} = 1.8 \times 10^4 \text{ ohm}$. At this field the resistivity does not depend on the temperature, i.e., $d\rho_{xx}/dT$ changes from positive to negative. Such crossing is often interpreted as a metal-to-insulator transition. In other words, the metallic state is suppressed by fields higher than 7.2 T. In the sample with $p=2 \times 10^{11} \text{ cm}^{-2}$ the increase in the magnetoresistance is just three times in the field range of 0–18 T (see Fig. 1). Over the entire range of the magnetic field used in the experiments this sample shows a metallic behavior as $d\rho_{xx}/dT > 0$.

As seen in Fig. 1 the resistance increase $[\rho_{xx}(12 \text{ T}) - \rho_{xx}(0)]/\rho_{xx}(0) \approx 50\%$ was observed¹⁴ on a sample with $p=2.5 \times 10^{11} \text{ cm}^{-2}$. That system also was in a metallic state in the fields of up to $B_{||}=12 \text{ T}$ used in Ref. 14.

In Fig. 2 the same magnetoresistance data obtained on the sample with $p=8.2 \times 10^{10} \text{ cm}^{-2}$ are replotted as the dependencies $\rho_{xx}(T)$ at several field values to clarify the modification of the $d\rho_{xx}/dT$ and its sign change at the field of 7.2 T.

The samples were mounted on a one axis rotator.¹⁶ That allowed determining the sample position at which the field was aligned parallel to the quantum well plane with an error of less than 10 min. Figure 3 illustrates the effect of sample rotation on the resistivity ρ_{xx} . The angle $\Theta=0^\circ$ corresponding to the precise alignment of the magnetic field parallel to the 2D-channel plane was determined at the ρ_{xx} maximal value.

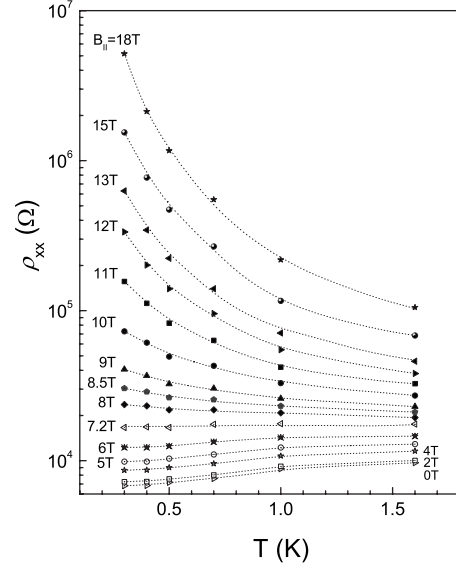


FIG. 2. Resistivity ρ_{xx} as a function of temperature T for different magnetic fields for the sample with $p=8.2 \times 10^{10} \text{ cm}^{-2}$ in configuration $B_{||} \perp I$.

By rotating the sample in a constant $B_{||}$, a perpendicular field component is induced. That leads to appearance of the Shubnikov-de Haas (SdH) oscillations. The oscillations pattern allows tracking the concentration change with, for instance, magnetic field intensity $B_{||}$. As seen in Fig. 3, with decrease in parallel component of applied magnetic field, the position of SdH oscillations shifts to larger angles. However, if to replot ρ_{xx} against the normal component of magnetic field B_{\perp} (see inset in Fig. 3), it appears that the oscillations minima for every $B_{||}$ are at the same B_{\perp} . If the positive magnetoresistance is determined by spin effects, then in the tilted field the structure of the SdH oscillations should depend on intensity of the parallel field $B_{||}$. If $B_{||}$ is less than the field, corresponding to a totally polarized electron system B_c , there is either appearance of oscillations with another period³ or a

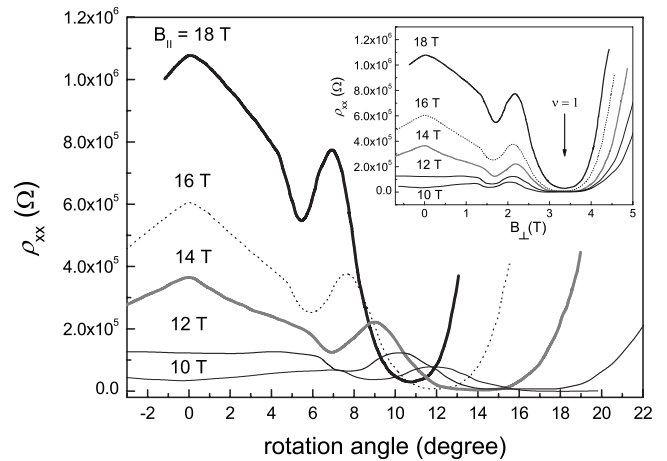


FIG. 3. Resistance ρ_{xx} as a function of the field tilting angle Θ with respect to the plane of the 2D layer at different magnetic fields $B_{||}$; $p=8.2 \times 10^{10} \text{ cm}^{-2}$, $B_{||} || I$. Inset: ρ_{xx} as a function of a magnetic field B_{\perp} , the normal component of the magnetic field.

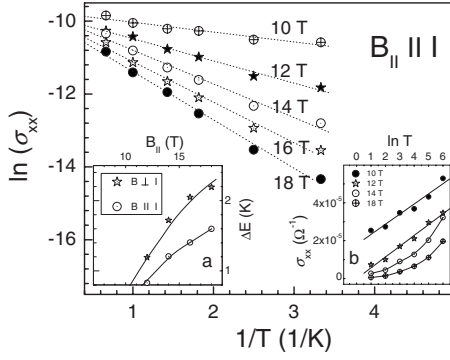


FIG. 4. Arrhenius plot of the p -Si/SiGe conductivity at different magnetic fields B_{\parallel} ; $p=8.2 \times 10^{10} \text{ cm}^{-2}$. Insets: (a) Activation energy as a function of in-plane magnetic field; (b) σ_{xx} vs $\ln T$.

change in B_{\perp} position of the oscillations minima, corresponding to the lower spin subband, until the magnetic field achieves the point of total spin polarization.² These facts are indicative of the two spin subbands repopulation with increase in the in-plane magnetic field B_{\parallel} till B_c .

According to our results (Fig. 3) in the fields $B > 10$ T nothing happens to position of the oscillations. This may support our interpretation that spin subbands are not formed. Another explanation would be that $B_c < 10$ T. The dependence $\rho_{xx}(B_{\parallel})$ presented in Fig. 1 shows pronounce increase with magnetic field without any trend to saturation. Thus explanation of such increase even assuming that $B > B_c$ would require account of orbital effects.

The temperature dependence of the conductivity σ_{xx} is plotted in Fig. 4. At $B > 12$ T this dependence has an activation character: $\sigma_{xx} \propto \exp[-\Delta E(B)/k_B T]$, with the activation energy ΔE depending on the in-plane magnetic field. The activationlike temperature dependence at $B_{\parallel} > 12$ T is a characteristic of the hole freezing-out on localized states. The corresponding conductance mechanism could be the nearest-neighbor hopping. The process of magnetic freezing-out is associated with sufficiently high magnetic fields where the wave-function deformation takes place. The inset (a) in Fig. 4 shows that for different orientations this deformation occurs in different ways: it is stronger for the $B_{\parallel} \perp I$ configuration than for $B_{\parallel} || I$ one.

However, in the field region of 7–12 T the holes conductivity mechanism could be hardly identified. Indeed, the temperature dependence of conductivity could be interpreted as activation with the energy $\Delta E \propto k_B T$ (see Fig. 4), and corresponding conductance mechanism could be the nearest-neighbor hopping. However, in the same magnetic field region the condition $\sigma_{xx} \propto \ln T$ is also valid [see inset (b) of Fig. 4], which could be expounded, for example, as quantum corrections to conductivity of the delocalized holes as done in Ref. 17.

To specify the conductivity mechanisms of charge carriers (holes) in parallel magnetic fields higher than 7.2 T, it is useful to compare the conductivity on a direct current with the high-frequency conductivity. In the present work the ac conductivity, being generally a complex function $\sigma^{ac} \equiv \sigma_1 - i\sigma_2$, has been measured on the same samples by acoustic methods. The acoustic technique involves measure-

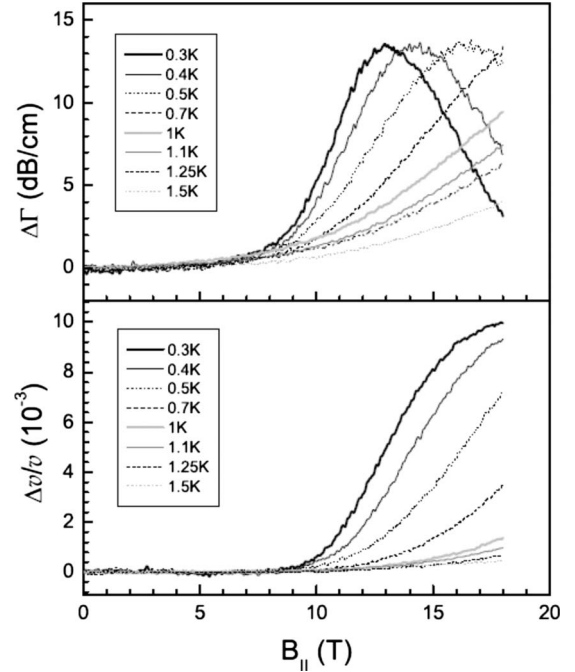


FIG. 5. Magnetic field dependences of $\Delta\Gamma(B_{\parallel})$ and $\Delta v(B_{\parallel})/v(0)$ for different temperatures. $f=17$ MHz, $p=8.2 \times 10^{10} \text{ cm}^{-2}$, and $k \perp B_{\parallel}$.

ments of the acoustoelectric effects: the variations in the velocity $\Delta v/v(0)=[v(B)-v(0)]/v(0)$ and the attenuation $\Delta\Gamma=\Gamma(B)-\Gamma(0)$ of a surface acoustic wave (SAW) [$\Gamma(0)$, $v(0)$ are the absorption and velocity at $B=0$, respectively] in the in-plane magnetic field of up to 18 T at temperatures 0.3–2 K. The measurements were performed in the frequency range of $f=17$ –157 MHz. Simultaneous measurements $\Delta v/v(0)$ and $\Delta\Gamma$ allow determining real σ_1 and imaginary σ_2 components of the ac conductivity σ^{ac} in the probeless way. As Ge and Si are not piezoelectric materials, the hybrid method was used. According to this technique the SAW is generated and propagates on a surface of a piezoelectric LiNbO₃ plate, while the sample is slightly pressed to the plate by springs. Thus, the electric field, accompanying the SAW and having the same frequency, penetrates the sample and interacts with the holes in a quantum well. In this configuration of the experiment no deformation is transmitted into the sample. Ac measurements were also conducted in two configurations: $k || B_{\parallel}$ and $k \perp B_{\parallel}$, where k is the SAW wave vector.

Shown in Fig. 5 are the parallel magnetic field dependences of the acoustic attenuation, $\Delta\Gamma(B_{\parallel})$, and velocity shift, $\Delta v(B_{\parallel})/v(0)$ at $f=17$ MHz, at different temperatures. The curves measured at other frequencies (30, 90, and 157 MHz) are similar to the ones presented in Fig. 5.

The components $\sigma_{1,2}$ can be found from simultaneous measurements of $\Delta\Gamma$ and $\Delta v/v(0)$ by solving the set of equations

$$\Delta\Gamma \propto \frac{\Sigma_1}{[1 + \Sigma_2]^2 + \Sigma_1^2}, \quad \frac{\Delta v}{v(0)} \propto \frac{1 + \Sigma_2}{[1 + \Sigma_2]^2 + \Sigma_1^2},$$

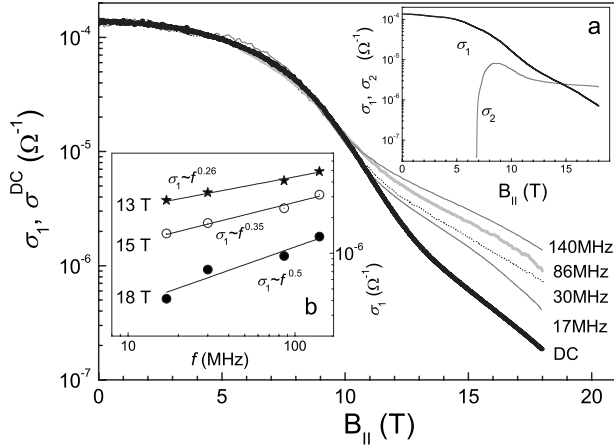


FIG. 6. Real part of the ac conductivity, σ_1 at different frequencies and dc conductivity versus in-plane magnetic field; $T=0.3$ K. Inset (a): real, σ_1 , and imaginary, σ_2 , components of the complex ac conductivity for $f=86$ MHz. Inset (b): frequency dependences of σ_1 at different magnetic fields, $T=0.3$ K.

$$\Sigma_1 \propto \sigma_1, \Sigma_2 \propto \sigma_2. \quad (1)$$

The detailed procedure of determination of the components σ_1 and σ_2 from acoustical measurements is described in Ref. 18.

Figure 6 illustrates experimental dependencies of the real component σ_1 of the complex ac conductivity, derived from the acoustical measurements at different frequencies using Eqs. (1), as well as the dc conductivity, on in-plane field. Inset (a) displays the σ_1 and σ_2 , measured at frequency $f=86$ MHz as a function of in-plane field. Inset (b) shows the frequency dependence of σ_1 at different magnetic fields.

The ratio between σ^{dc} , σ_1 , and σ_2 is crucial in determination of the conductivity mechanism. If charge carriers (holes) find themselves in delocalized states the ac and dc conductivity mechanisms are the same, and $\sigma^{\text{dc}} = \sigma^{\text{ac}} = \sigma_1$, while the imaginary part $\sigma_2 = 0$.¹⁹ It is seen in Fig. 6, that ac and dc conductivities coincide in the fields of up to $B_{\parallel} \approx 11-12$ T. As is also obvious from the figure, the magnetic field, at which σ^{dc} and σ_1 start to diverge, depends on a frequency: the higher the frequency the less this field.

The ac and dc conductivities up to $B_{\parallel} \approx 11-12$ T are due to delocalized holes. At $B_{\parallel} > 12$ T a localization of the charge carriers begins, resulting in the nearest-neighbor hopping in the dc and the “two-site” hopping ac conductivity.²⁰ The latter is characterized by a frequency dependence of σ_1 [see inset (b) in Fig. 6] and emergence of the imaginary component σ_2 [see inset (a) in Fig. 6]. Moreover, as seen in inset (a) of Fig. 6, at fields $B_{\parallel} > 15$ T the ratio $\sigma_2 > \sigma_1$ is valid, which is typical of the “two-site” hopping for two-dimensional systems.²¹

According to these results, at $B_{\parallel} > 12$ T the charge carriers are localized and the conductance is due to hopping. It supports the conclusion that near $B_{\parallel} = 7.2$ T the hole states are seemingly extended up to $B_{\parallel} \approx 12$ T. Consequently, temperature dependence of conductivity is most likely determined by interplay between weak localization and $e-e$ interactions. In this paper we do not focus on detailed study of the

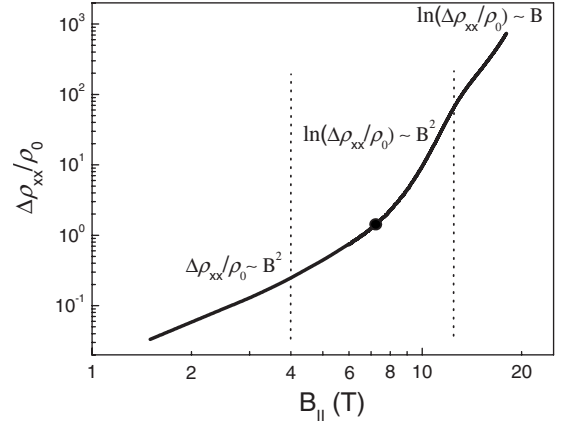


FIG. 7. Dependence of $\Delta\rho_{xx}/\rho_0$ on B_{\parallel} at $T=0.3$ K for the sample with $p=8.2 \times 10^{10}$ cm⁻². $B_{\parallel} \perp I$.

conductivity in the vicinity of $B_{\parallel} = 7.2$ T because of the small variation in conductivity with temperature and narrow available temperature interval.

We now consider the magnetic field dependence of the magnetoresistance shown in Fig. 7. The single point on the curve corresponds to $B_{\parallel} = 7.2$ T. On the metallic side until $B_{\parallel} = 4$ T the magnetoresistance obeys a power law $\Delta\rho_{xx}/\rho_0 \propto B^2$. In the fields below 13 T the resistivity follows a law $\ln(\Delta\rho_{xx}/\rho_0) \propto B^2$, but then at $B_t \approx 13$ T a transition to a dependence $\ln(\Delta\rho_{xx}/\rho_0) \propto B$ occurs.

III. SUMMARY

The principal experimental facts revealed in this study are the following:

(1) An in-plane magnetic field induces a giant positive magnetoresistance (with no sign of saturation) in p -Si/SiGe heterostructures. This effect is observed in the system with lowest density ($p=8.2 \times 10^{10}$ cm⁻²) only. When the magnetic field rises up to 18 T, the resistivity in this sample increases significantly and changes by more than three orders of magnitude, while in the sample with $p=2 \times 10^{11}$ cm⁻² the magnetoresistance increase is just several times in the same field range.

(2) In the sample with $p=8.2 \times 10^{10}$ cm⁻² the derivative $d\rho_{xx}/dT$ changes its sign at $B \approx 7.2$ T. It could be interpreted as a magnetic field suppression of the metallic state. In the sample with $p=2 \times 10^{11}$ cm⁻² the sign change of $d\rho_{xx}/dT$ was not observed.

(3) The magnetoresistance in p -Si/SiGe heterostructure with $p=8.2 \times 10^{10}$ cm⁻² is anisotropic: it depends on orientation of the current with respect to the in-plane magnetic field, $B_{\parallel} \perp I$ or $B_{\parallel} \parallel I$. At $B_{\parallel} = 18$ T and $T=0.3$ K the resistivity ratio $\rho_{xx}^{B \perp I} / \rho_{xx}^{B \parallel I}$ equals 3.

(4) In the sample with $p=8.2 \times 10^{10}$ cm⁻² at $B_t \approx 13$ T a transition from the law $\ln(\Delta\rho_{xx}/\rho_0) \propto B^2$ to $\ln(\Delta\rho_{xx}/\rho_0) \propto B$ was observed.

All these experimental facts could be explained qualitatively using the theory developed in Ref. 10. Authors of Ref. 10 neglect spin-related effects and consider the in-plane magnetoresistance as affected by the charge-carrier orbital motion in the wide quantum well.

The theory¹⁰ is applicable if the following two conditions are met:

(a) The magnetic length $l_B = \sqrt{\hbar c / eB}$ is less than the 2D layer thickness Z : $Z \gg l_B$.

If one is to assume that the quantum well bottom is distorted weakly, one may hold $Z \sim 3 \times 10^{-6}$ cm. Then the magnetic length l_B becomes less than thickness of 2D layer and condition (a) is fulfilled already at $B_{\parallel} \cong 1$ T.

(b) The 2D Fermi wavelength l_F at $B=0$ is substantially larger than the magnetic length $\lambda_F \gg l_B$, where $\lambda_F = \frac{2\pi}{k_F}$; $k_F = (2\pi p)^{1/2}$, which is also valid in our experiments.

The theory¹⁰ predicts (i) a large positive magnetoresistance in systems with low carrier density; (ii) a large anisotropy of resistivity in the 2D plane $\rho^{\perp} \gg \rho^{\parallel}$; (iii) a reduction in the effect with increasing density; and (iv) a change in the $\rho(B)$ dependence: at low B ($\omega_c < \omega_0$), $\ln(\rho_{xx}) \propto B^2$, at high B ($\omega_c > \omega_0$), $\ln(\rho_{xx}) \propto B$, where $\hbar\omega_0$ is the subband splitting, and ω_c is the cyclotron frequency. All these predictions (i)–(iv) seem to be consistent with the obtained experimental data.

Thus, one can calculate the thickness of the 2D well if the $B_{\parallel} \cong 13$ T value is known. The transition occurs when

$$\omega_0 = \omega_c; \omega_0 = \frac{\Delta E}{\hbar} = \frac{(E_2 - E_1)}{\hbar}; \omega_c = \frac{eB}{m^*c}, \quad (2)$$

where E_1 are E_2 are the energies of first and second levels of dimensional quantization and $E_n = \frac{\hbar^2 \pi^2 n^2}{2m^* Z^2}$, where n is the number of the dimensional quantization band.

It follows from Eq. (2) that

$$Z^2 = (n_2^2 - n_1^2)(\pi^2 \hbar c) / (2eB_{\parallel}). \quad (3)$$

A calculation with Eq. (3) gives $Z = 2.7 \times 10^{-6}$ cm, which is consistent with the nominal thickness of the SiGe layer in the studied 2D hole system: $Z = 3 \times 10^{-6}$ cm. It should be noted that Eq. (3) provides only a rough estimation of Z because a field dependence of E_n is not taken into account there.

In conclusion, the large positive magnetoresistance in the parallel magnetic field increases most likely due to interaction of the in-plane field with the carrier orbital motion in the quasi-2D layer with finite thickness and can be qualitatively explained by the theory.¹⁰ The absence of a strong effect of the in-plane magnetic field on the resistivity in Ref. 14 can be possibly attributed to the relatively high carrier density in the system studied there. This is consistent with our data obtained on the sample with $p = 2 \times 10^{11}$ cm⁻².

ACKNOWLEDGMENTS

Authors are grateful to Y.M. Galperin, L. Golub, M. Glazov, and G. Min'kov for useful discussions, and to E. Palm and T. Murphy for their help with the experiments. This work was supported by RFBR under Grant No. 08-02-00852; the Presidium of the Russian Academy of Science, the Program of Branch of Physical Sciences of RAS "Spintronika," by the NSF through Cooperative Agreement No. DMR-0084173, the State of Florida, and the DOE.

*ivan.smirnov@mail.ioffe.ru

¹D. Simonian, S. V. Kravchenko, M. P. Sarachik, and V. M. Pudalov, Phys. Rev. Lett. **79**, 2304 (1997); A. A. Shashkin, E. V. Deviatov, V. T. Dolgoplov, A. A. Kapustin, S. Anissimova, A. Venkatesan, S. V. Kravchenko, and T. M. Klapwijk, Phys. Rev. B **73**, 115420 (2006).

²T. Okamoto, M. Ooya, K. Hosoya, and S. Kawaji, Phys. Rev. B **69**, 041202 (2004); K. Lai, W. Pan, D. C. Tsui, S. A. Lyon, M. Muhlberger, and F. Schaffler, *ibid.* **72**, 081313(R) (2005).

³E. Tutuc, S. Melinte, and M. Shayegan, Phys. Rev. Lett. **88**, 036805 (2002); E. Tutuc, E. P. De Poortere, S. J. Papadakis, and M. Shayegan, *ibid.* **86**, 2858 (2001); Physica E **13**, 748 (2002).

⁴X. P. A. Gao, G. S. Boebinger, A. P. Mills Jr., A. P. Ramirez, L. N. Pfeiffer, and K. W. West, Phys. Rev. B **73**, 241315(R) (2006).

⁵J. Yoon, C. C. Li, D. Shahar, D. C. Tsui, and M. Shayegan, Phys. Rev. Lett. **84**, 4421 (2000).

⁶V. T. Dolgoplov and A. Gold, Pis'ma Zh. Eksp. Teor. Fiz. **71**, 42 (2000) [JETP Lett. **71**, 27 (2000)].

⁷B. Spivak, Phys. Rev. B **67**, 125205 (2003).

⁸P. Phillips, Yi Wan, I. Martin, S. Knysh, and D. Davidovich, Nature (London) **395**, 253 (1998).

⁹G. Zala, B. N. Narozhny, and I. L. Aleiner, Phys. Rev. B **64**, 214204 (2001).

¹⁰S. Das Sarma and E. H. Hwang, Phys. Rev. Lett. **84**, 5596 (2000).

¹¹T. P. Pearsall, F. H. Pollak, J. C. Bean, and R. Hull, Phys. Rev. B **33**, 6821 (1986).

¹²E. Glaser, J. M. Trombetta, T. A. Kennedy, S. M. Prokes, O. J. Glembocki, K. L. Wang, and C. H. Chern, Phys. Rev. Lett. **65**, 1247 (1990).

¹³E. Abrahams, S. V. Kravchenko, and M. P. Sarachik, Rev. Mod. Phys. **73**, 251 (2001).

¹⁴S. I. Dorozhkin, C. J. Emeleus, T. E. Whall, and G. Landwehr, Phys. Rev. B **52**, R11638 (1995).

¹⁵I. L. Drichko, A. M. Dyakonov, I. Yu. Smirnov, A. V. Suslov, Y. M. Galperin, V. Vinokur, M. Myronov, O. A. Mironov, and D. R. Leadley, Phys. Rev. B **77**, 085327 (2008).

¹⁶E. C. Palm and T. P. Murphy, Rev. Sci. Instrum. **70**, 237 (1999).

¹⁷X. P. A. Gao, A. P. Mills, Jr., A. P. Ramirez, L. N. Pfeiffer, and K. W. West, Phys. Rev. Lett. **89**, 016801 (2002); **88**, 166803 (2002).

¹⁸I. L. Drichko, A. M. Diakonov, I. Yu. Smirnov, Yu. M. Galperin, and A. I. Toropov, Phys. Rev. B **62**, 7470 (2000).

¹⁹I. L. Drichko, A. M. Diakonov, A. M. Kreshchuk, T. A. Polyan-skaya, I. G. Savel'ev, I. Yu. Smirnov, and A. V. Suslov, Fiz. Tekh. Poluprovodn. (S.-Peterburg) **31**, 451 (1997) [Semiconductors **31**, 384 (1997)].

²⁰M. Pollak and T. H. Geballe, Phys. Rev. **122**, 1742 (1961).

²¹A. L. Efros, Zh. Eksp. Teor. Fiz. **89**, 1834 (1985) [Sov. Phys. JETP **62**, 1057 (1985)].